11

Single-phase Controlled Rectifiers

José Rodríguez, Ph.D., Pablo Lezana, Samir Kouro, and Alejandro Weinstein
Department of Electronics, Universidad Técnica Federico Santa María, Valparaíso, Chile

11.1 Introduction

This chapter is dedicated to single-phase controlled rectifiers, which are used in a wide range of applications. As shown in Fig. 11.1, single-phase rectifiers can be classified into two big categories:

(i) Topologies working with low switching frequency, also known as line commutated or phase controlled rectifiers.
(ii) Circuits working with high switching frequency, also known as power factor correctors (PFCs).

Line-commutated rectifiers with diodes, covered in a previous chapter of this handbook, do not allow the control of power being converted from ac to dc. This control can be achieved with the use of thyristors. These controlled rectifiers are addressed in the first part of this chapter.

In the last years, increasing attention has been paid to the control of current harmonics present at the input side of the rectifiers, originating from a very important development in the so-called PFC. These circuits use power transistors working with high switching frequency to improve the waveform quality of the input current, increasing the power factor. High power factor rectifiers can be classified in regenerative and non-regenerative topologies and they are covered in the second part of this chapter.

11.2 Line-commutated Single-phase Controlled Rectifiers

11.2.1 Single-phase Half-wave Rectifier

The single-phase half-wave rectifier uses a single thyristor to control the load voltage as shown in Fig. 11.2. The thyristor will conduct, on-state, when the voltage v_T is positive and a firing current pulse i_G is applied to the gate terminal. The control of the load voltage is performed by delaying the firing pulse by an angle α. The firing angle α is measured from the position where a diode would naturally conduct. In case of Fig. 11.2 the angle α is measured from the zero-crossing point of the supply voltage v_s. The load in Fig. 11.2 is resistive and therefore the current i_d has the same waveform of the load voltage. The thyristor goes to the non-conducting condition, off-state, when the load voltage, and consequently the current, reaches a negative value.

The load average voltage is given by

$$V_{d\alpha} = \frac{1}{2\pi}\int_{\alpha}^{\pi} V_{max}\sin(\omega t)d(\omega t) = \frac{V_{max}}{2\pi}(1+\cos\alpha) \tag{11.1}$$

where V_{max} is the supply peak voltage. Hence, it can be seen from Eq. (11.1) that changing the firing angle α controls

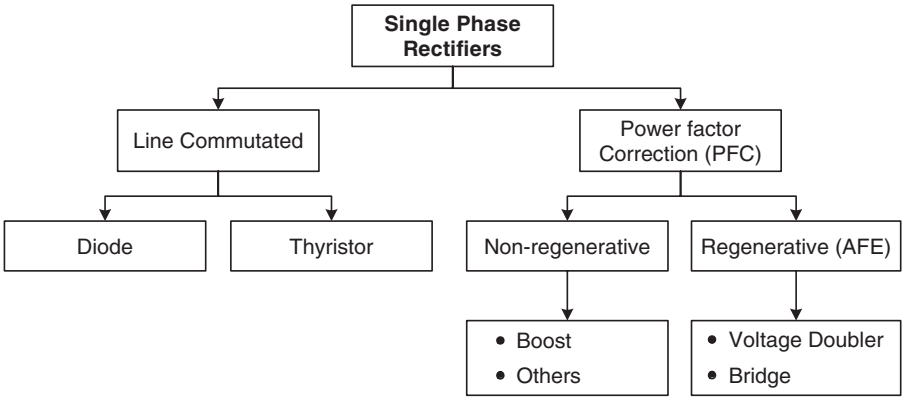

FIGURE 11.1 Single-phase rectifier classification.

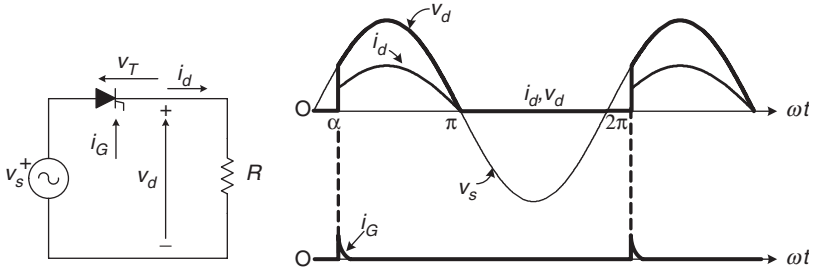

FIGURE 11.2 Single-thyristor rectifier with resistive load.

both the load average voltage and the amount of transferred power.

Figure 11.3a shows the rectifier waveforms for an *R–L* load. When the thyristor is turned on, the voltage across the inductance is

$$v_L = v_s - v_R = L\frac{di_d}{dt} \tag{11.2}$$

where v_R is the voltage in the resistance *R*, given by $v_R = R \cdot i_d$. If $v_s - v_R > 0$, from Eq. (11.2) holds that the load current increases its value. On the other hand, i_d decreases its value when $v_s - v_R < 0$. The load current is given by

$$i_d(\omega t) = \frac{1}{\omega L}\int_{\alpha}^{\omega t} v_L \, d\theta \tag{11.3}$$

Graphically, Eq. (11.3) means that the load current i_d is equal to zero when $A_1 = A_2$, maintaining the thyristor in conduction state even when $v_s < 0$.

When an inductive–active load is connected to the rectifier, as illustrated in Fig. 11.3b, the thyristor will be turned on if the firing pulse is applied to the gate when $v_s > E_d$. Again, the thyristor will remain in the on-state until $A_1 = A_2$. When the thyristor is turned off, the load voltage will be $v_d = E_d$.

11.2.2 Bi-phase Half-wave Rectifier

The bi-phase half-wave rectifier, shown in Fig. 11.4, uses a center-tapped transformer to provide two voltages v_1 and v_2. These two voltages are 180° out of phase with respect to the mid-point neutral *N*. In this scheme, the load is fed via thyristors T_1 and T_2 during each positive cycle of voltages v_1 and v_2, respectively, while the load current returns via the neutral *N*.

As illustrated in Fig. 11.4, thyristor T_1 can be fired into the on-state at any time while voltage $v_{T1} > 0$. The firing pulses are delayed by an angle α with respect to the instant where diodes would conduct. Also the current paths for each conduction state are presented in Fig. 11.4. Thyristor T_1 remains in the on-state until the load current tends to a negative value. Thyristor T_2 is fired into the on-state when $v_{T2} > 0$, which corresponds in Fig. 11.4 to the condition when $v_2 > 0$.

The mean value of the load voltage with resistive load is determined by

$$V_{di\alpha} = \frac{1}{\pi}\int_{\alpha}^{\pi} V_{max}\sin(\omega t)d(\omega t) = \frac{V_{max}}{\pi}(1+\cos\alpha) \tag{11.4}$$

The ac supply current is equal to $i_{T1}(N_2/N_1)$ when T_1 is in the on-state and $-i_{T2}(N_2/N_1)$ when T_2 is in the on-state, where N_2/N_1 is the transformer turns ratio.

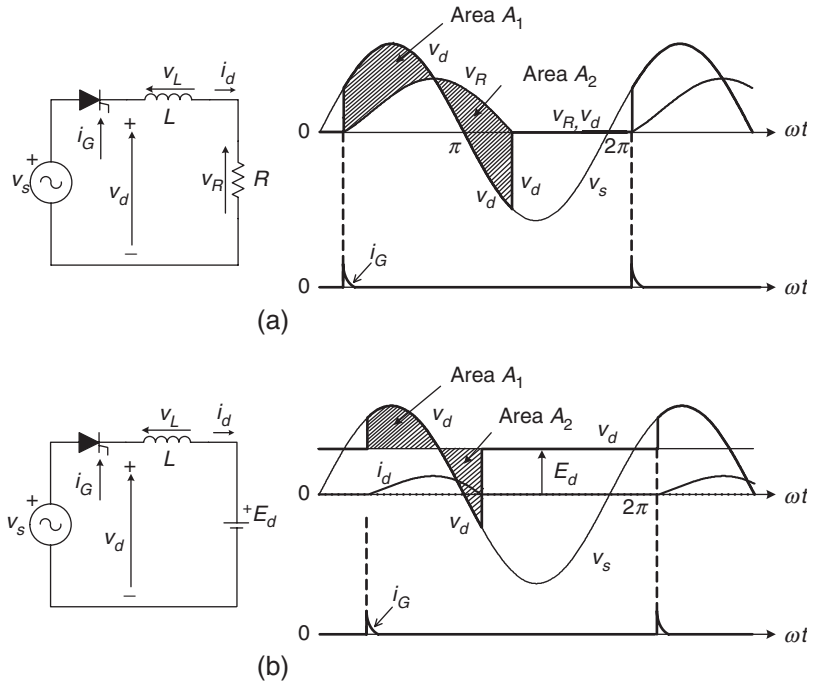

FIGURE 11.3 Single-thyristor rectifier with: (a) resistive-inductive load and (b) active load.

The effect of the load time constant $T_L = L/R$, on the normalized load current $i_d(t)/i_R(t)$ for a firing angle $\alpha = 0°$ is shown in Fig. 11.5. The ripple in the load current reduces as the load inductance increases. If the load inductance $L \to \infty$, then the current is perfectly filtered.

11.2.3 Single-phase Bridge Rectifier

Figure 11.6a shows a fully controlled bridge rectifier, which uses four thyristors to control the average load voltage. In addition, Fig. 11.6b shows the half-controlled bridge rectifier which uses two thyristors and two diodes.

The voltage and current waveforms of the fully controlled bridge rectifier for a resistive load are illustrated in Fig 11.7. Thyristors T_1 and T_2 must be fired on simultaneously during the positive half-wave of the source voltage v_s, to allow the conduction of current. Alternatively, thyristors T_3 and T_4 must be fired simultaneously during the negative half-wave of the source voltage. To ensure simultaneous firing, thyristors T_1 and T_2 use the same firing signal. The load voltage is similar to the voltage obtained with the bi-phase half-wave rectifier. The input current is given by

$$i_S = i_{T1} - i_{T4} \tag{11.5}$$

and its waveform is shown in Fig. 11.7.

Figure 11.8 presents the behavior of the fully controlled rectifier with resistive–inductive load (with $L \to \infty$). The high load inductance generates a perfectly filtered current and the rectifier behaves like a current source. With continuous load current, thyristors T_1 and T_2 remain in the on-state beyond the positive half-wave of the source voltage v_s. For this reason, the load voltage v_d can have a negative instantaneous value. The firing of thyristors T_3 and T_4 has two effects:

(i) they turn-off thyristors T_1 and T_2 and
(ii) after the commutation, they conduct the load current.

This is the main reason why this type of converters are called "naturally commutated" or "line commutated" rectifiers. The supply current i_S has the square waveform, as shown in Fig. 11.9, for continuous conduction. In this case, the average load voltage is given by

$$V_{di\alpha} = \frac{1}{\pi}\int_{\alpha}^{\pi+\alpha} V_{max}\sin(\omega t)d(\omega t) = \frac{2V_{max}}{\pi}\cos\alpha \tag{11.6}$$

11.2.4 Analysis of the Input Current

Considering a very high inductive load, the input current in a bridge-controlled rectifier is filtered and presents a square waveform. In addition, the input current i_s is shifted by the firing angle α with respect to the input voltage v_s, as shown in Fig. 11.9a. The input current can be expressed as a Fourier series, where the amplitude of the different harmonics are

$$I_{smax,\,n} = \frac{4}{\pi}\frac{I_d}{n} \quad (n = 1, 3, 5, \ldots) \tag{11.7}$$

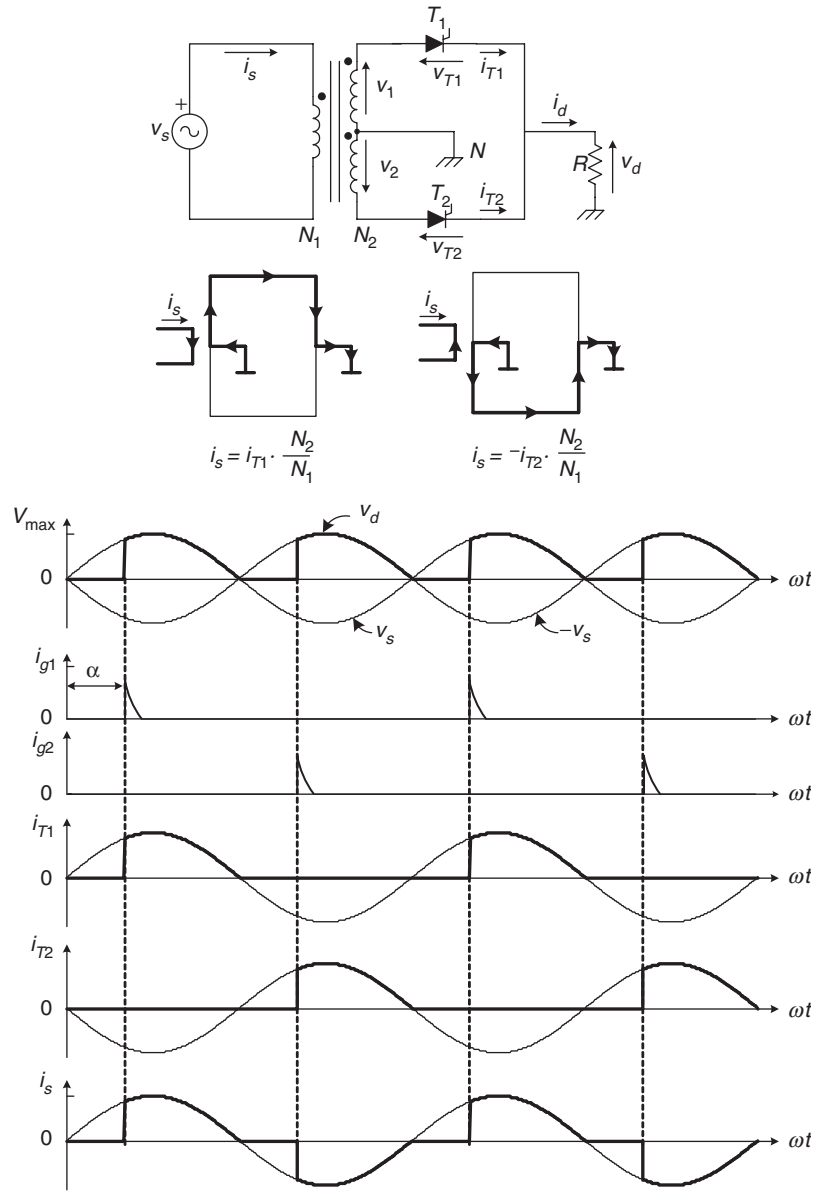

FIGURE 11.4 Bi-phase half-wave rectifier.

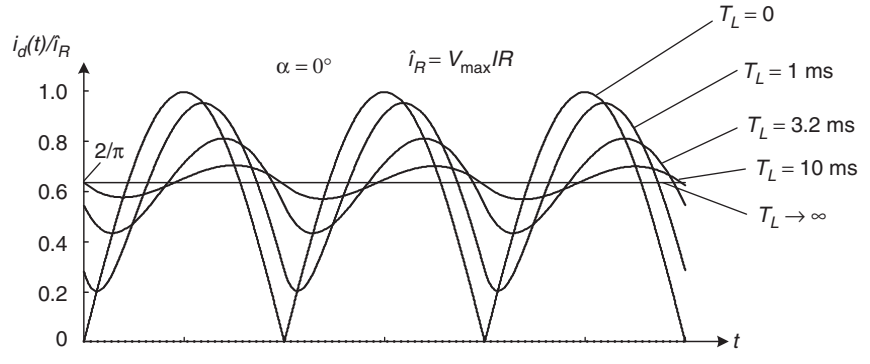

FIGURE 11.5 Effect of the load time constant over the current ripple.

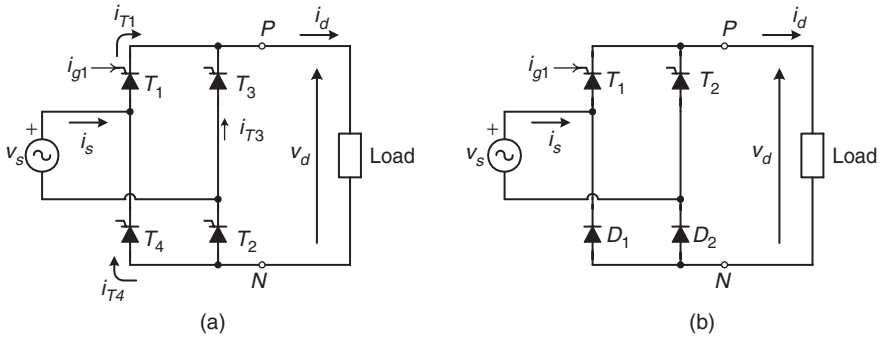

FIGURE 11.6 Single-phase bridge rectifier: (a) fully controlled and (b) half-controlled.

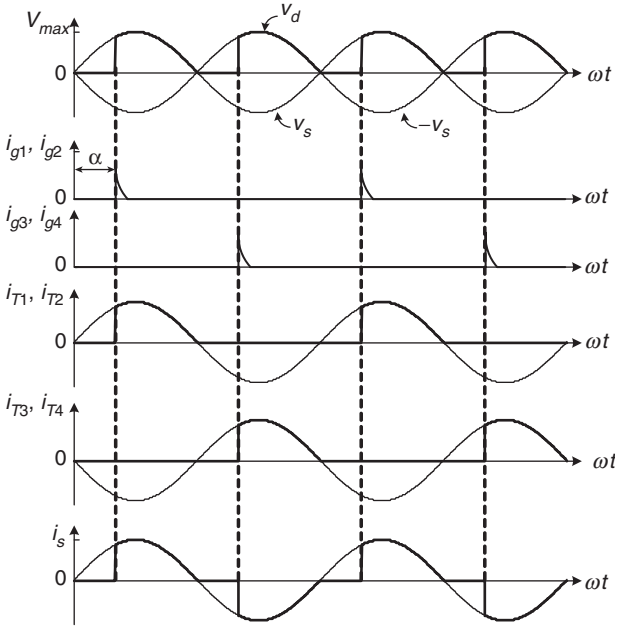

FIGURE 11.7 Waveforms of a fully controlled bridge rectifier with resistive load.

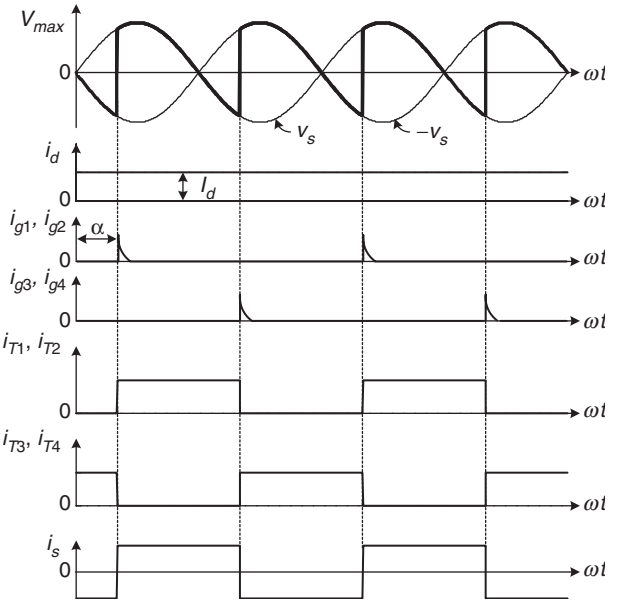

FIGURE 11.8 Waveforms of a fully controlled bridge rectifier with resistive–inductive load ($L \rightarrow \infty$).

where n is the harmonic order. The root mean square (rms) value of each harmonic can be expressed as

$$I_{sn} = \frac{I_{smax,\,n}}{\sqrt{2}} = \frac{2\sqrt{2}}{\pi}\frac{I_d}{n} \tag{11.8}$$

Thus, the rms value of the fundamental current i_{s1} is

$$I_{s1} = \frac{2\sqrt{2}}{\pi} I_d = 0.9 I_d \tag{11.9}$$

It can be observed from Fig. 11.9a that the displacement angle ϕ_1 of the fundamental current i_{s1} corresponds to the firing angle α. Figure 11.9b shows that in the harmonic spectrum of the input current, only odd harmonics are present with

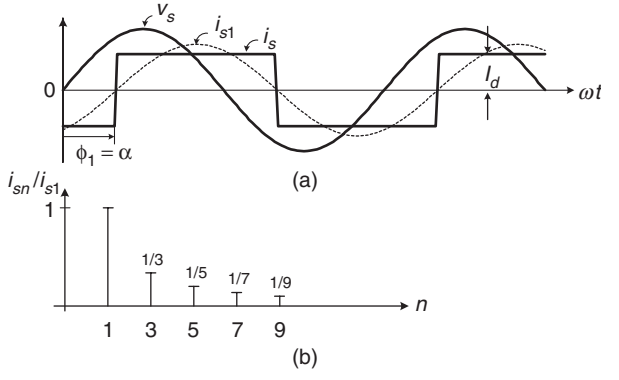

FIGURE 11.9 Input current of the single-phase controlled rectifier in bridge connection: (a) waveforms and (b) harmonics spectrum.

decreasing amplitude while the frequency increases. Finally the rms value of the input current i_s is

$$I_s = I_d \tag{11.10}$$

The total harmonic distortion (THD) of the input current can be determined by

$$\text{THD} = \frac{\sqrt{I_s^2 - I_{s1}^2}}{I_{s1}} 100 = 48.4\% \tag{11.11}$$

11.2.5 Power Factor of the Rectifier

The displacement factor of the fundamental current, obtained from Fig. 11.9a is

$$\cos\phi_1 = \cos\alpha \tag{11.12}$$

In the case of non-sinusoidal currents, the active power delivered by the sinusoidal single-phase supply is

$$P = \frac{1}{T}\int_0^T v_s(t) i_s(t) dt = V_s I_{s1} \cos\phi_1 \tag{11.13}$$

where V_s is the rms value of the single-phase voltage v_s.

The apparent power is given by

$$S = V_s I_s \tag{11.14}$$

The power factor (PF) is defined by

$$\text{PF} = \frac{P}{S} \tag{11.15}$$

Substitution from Eqs. (11.12), (11.13), and (11.14) in Eq. (11.15) yields

$$\text{PF} = \frac{I_{s1}}{I_s}\cos\alpha \tag{11.16}$$

This equation shows clearly that due to the non-sinusoidal waveform of the input current, the power factor of the rectifier is negatively affected both by the firing angle α and by the distortion of the input current. In effect, an increase in the distortion of the current produces an increase in the value of I_s in Eq. (11.16), which deteriorates the power factor.

11.2.6 The Commutation of the Thyristors

Until now, the current commutation between thyristors has been considered to be instantaneous. This condition is not valid in real cases due to the presence of the line inductance L, as shown in Fig. 11.10a. During the commutation, the current through the thyristors cannot change instantaneously, and for this reason, during the commutation angle μ, all four thyristors are conducting simultaneously. Therefore, during the commutation, the following relationship for the load voltage holds

$$v_d = 0 \quad \alpha \le \omega t \le \alpha + \mu \tag{11.17}$$

The effect of the commutation on the supply current, voltage waveforms, and the thyristor current waveforms can be observed in Fig. 11.10b.

During the commutation, the following expression holds

$$L\frac{di_s}{dt} = v_s = V_{max}\sin(\omega t) \quad \alpha \le \omega t \le \alpha + \mu \tag{11.18}$$

Integrating Eq. (11.18) over the commutation interval yields

$$\int_{-I_d}^{I_d} di_s = \frac{V_{max}}{L}\int_{\alpha/\omega}^{\alpha+\mu/\omega} \sin(\omega t) dt \tag{11.19}$$

From Eq. (11.19), the following relationship for the commutation angle μ is obtained

$$\cos(\alpha + \mu) = \cos\alpha - \frac{2\omega L}{V_{max}} I_d \tag{11.20}$$

Equation (11.20) shows that an increase of the line inductance L or an increase of the load current I_d increases the commutation angle μ. In addition, the commutation angle is affected by the firing angle α. In effect, Eq. (11.18) shows that with different values of α, the supply voltage v_s has a different instantaneous value, which produces different di_s/dt, thereby affecting the duration of the commutation.

Equation (11.17) and the waveform of Fig. 11.10b show that the commutation process reduces the average load voltage $V_{d\alpha}$. When the commutation is considered, the expression for the average load voltage is given by

$$V_{d\alpha} = \frac{1}{\pi}\int_{\alpha+\mu}^{\pi+\alpha} \sin(\omega t) d(\omega t) = \frac{V_{max}}{\pi}\left[\cos(\alpha+\mu) + \cos\alpha\right] \tag{11.21}$$

Substituting Eq. (11.20) into Eq. (11.21) yields

$$V_{d\alpha} = \frac{2}{\pi} V_{max}\cos\alpha - \frac{2\omega L}{\pi} I_d \tag{11.22}$$

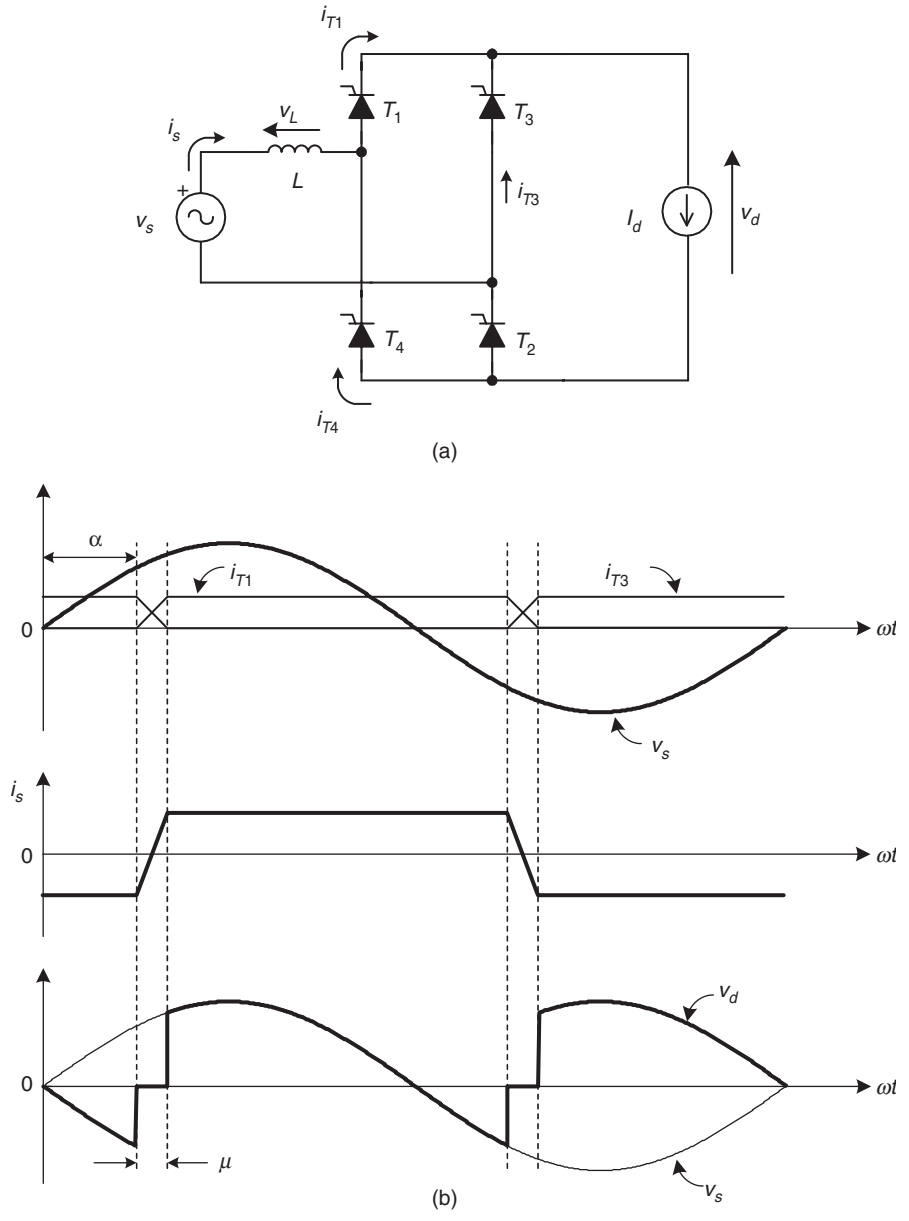

FIGURE 11.10 The commutation process: (a) circuit and (b) waveforms.

11.2.7 Operation in the Inverting Mode

When the angle $\alpha > 90°$, it is possible to obtain a negative average load voltage. In this condition, the power is fed back to the single-phase supply from the load. This operating mode is called inverter or inverting mode, because the energy is transferred from the dc to the ac side. In practical cases, this operating mode is obtained when the load configuration is as shown in Fig. 11.11a. It must be noticed that this rectifier allows unidirectional load current flow.

Figure 11.11b shows the waveform of the load voltage with the rectifier in the inverting mode, neglecting the source inductance L.

Section 11.2.6 described how supply inductance increases the conduction interval of the thyristors by the angle μ. As shown in Fig. 11.11c, the thyristor voltage v_{T1} has a negative value during the extinction angle γ, defined by

$$\gamma = 180 - (\alpha + \mu) \tag{11.23}$$

To ensure that the outgoing thyristor will recover its blocking capability after the commutation, the extinction angle should satisfy the following restriction

$$\gamma > \omega t_q \tag{11.24}$$

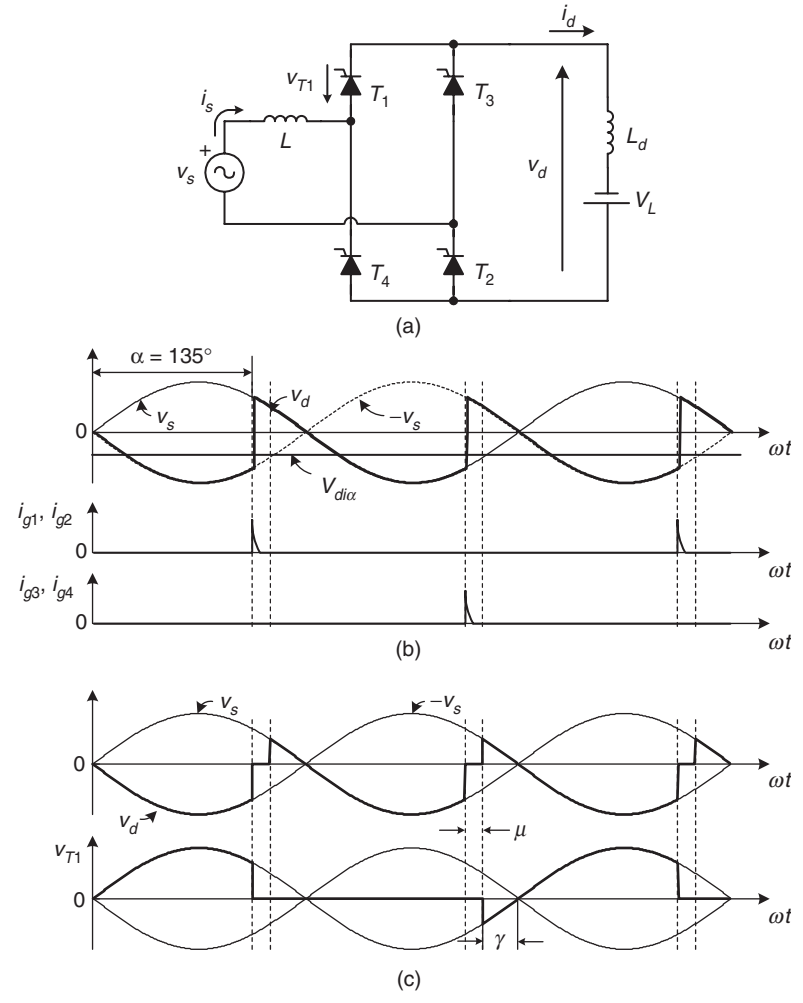

FIGURE 11.11 Rectifier in the inverting mode: (a) circuit; (b) waveforms neglecting source inductance L; and (c) waveforms considering L.

where ω is the supply frequency and t_q is the thyristor turn-off time. Considering Eqs. (11.23) and (11.24) the maximum firing angle is, in practice,

$$\alpha_{max} = 180 - \mu - \gamma \tag{11.25}$$

If the condition of Eq. (11.25) is not satisfied, the commutation process will fail, originating destructive currents.

11.2.8 Applications

Important application areas of controlled rectifiers include uninterruptible power supplies (UPS), for feeding critical loads. Figure 11.12 shows a simplified diagram of a single-phase UPS configuration, typically rated for <10 kVA. A fully controlled or half-controlled rectifier is used to generate the dc voltage for the inverter. In addition, the input rectifier acts as a battery charger. The output of the inverter is filtered before it is fed to the load. The most important operation modes of the UPS are:

(i) Normal mode. In this case the line voltage is present. The critical load is fed through the rectifier-inverter scheme. The rectifier keeps the battery charged.
(ii) Outage mode. During a loss of the ac main supply, the battery provides the energy for the inverter.
(iii) Bypass operation. When the load demands an over-current to the inverter, the static bypass switch is turned on and the critical load is fed directly from the mains.

The control of low power dc motors is another interesting application of controlled single-phase rectifiers. In the circuit of Fig. 11.13, the controlled rectifier regulates the armature voltage and consequently controls the motor current i_d in order to produce a required torque.

This configuration allows only positive current flow in the load. However the load voltage can be both positive

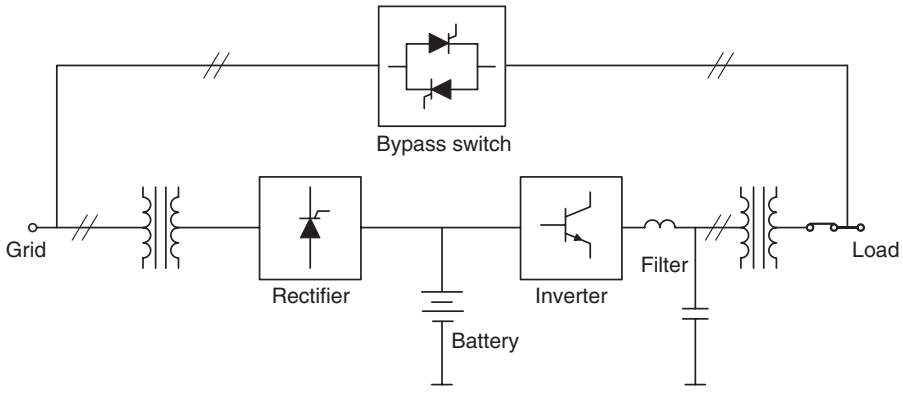

FIGURE 11.12 Application of a rectifier in single-phase UPS.

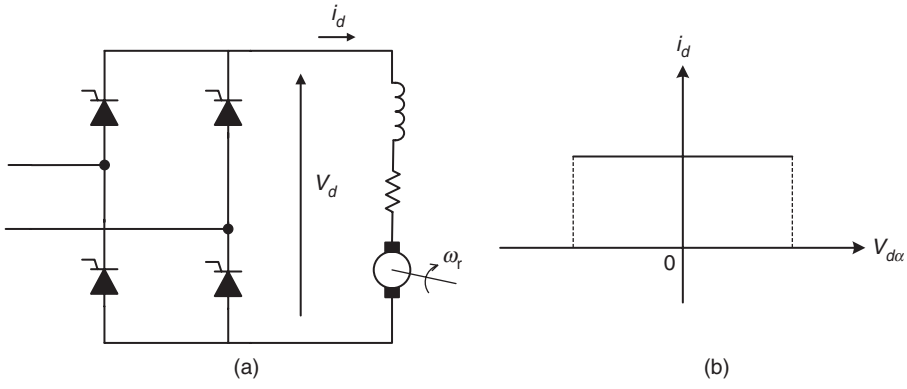

FIGURE 11.13 Two-quadrant dc drive: (a) circuit and (b) quadrants of operation.

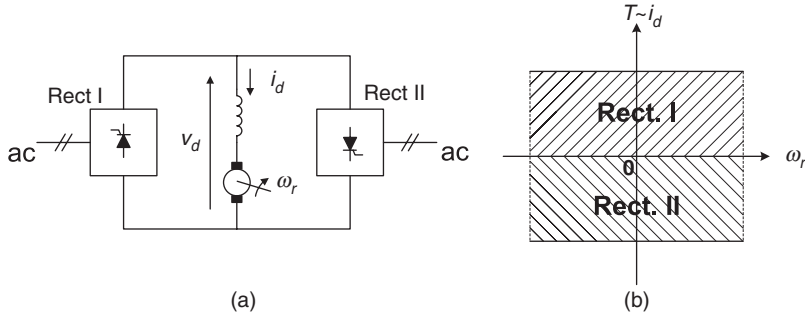

FIGURE 11.14 Single-phase dual-converter drive: (a) connection and (b) four-quadrant operation.

and negative. For this reason, this converter works in the two-quadrant mode of operation in the plane i_d vs $V_{d\alpha}$.

A better performance can be obtained with two rectifiers in back-to-back connection at the dc terminals, as shown in Fig. 11.14a. This arrangement, known as a dual converter configuration, allows four-quadrant operation of the drive. Rectifier I provides positive load current i_d, while rectifier II provides negative load current. The motor can work in forward powering, forward braking (regenerating), reverse powering, and reverse braking (regenerating). These operating modes are shown in Fig. 11.14b, where the torque T vs the rotor speed ω_r is illustrated.

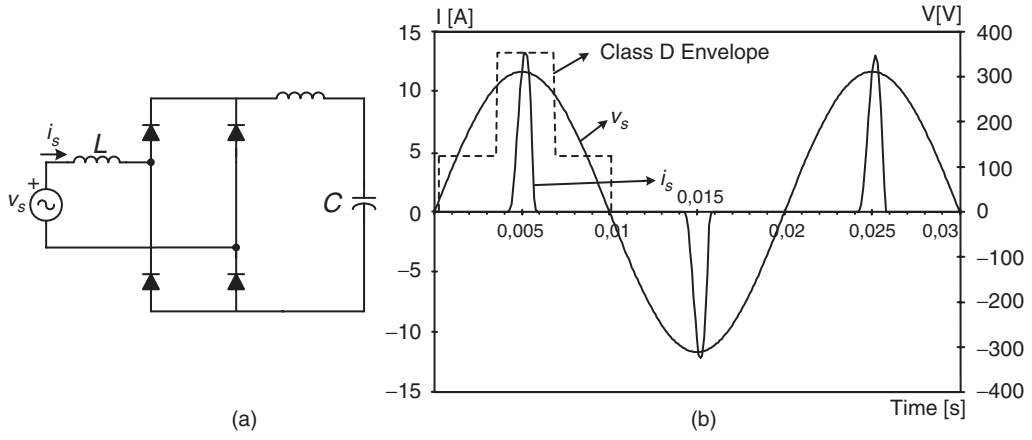

FIGURE 11.15 Single-phase rectifier: (a) circuit and (b) waveforms of the input voltage and current.

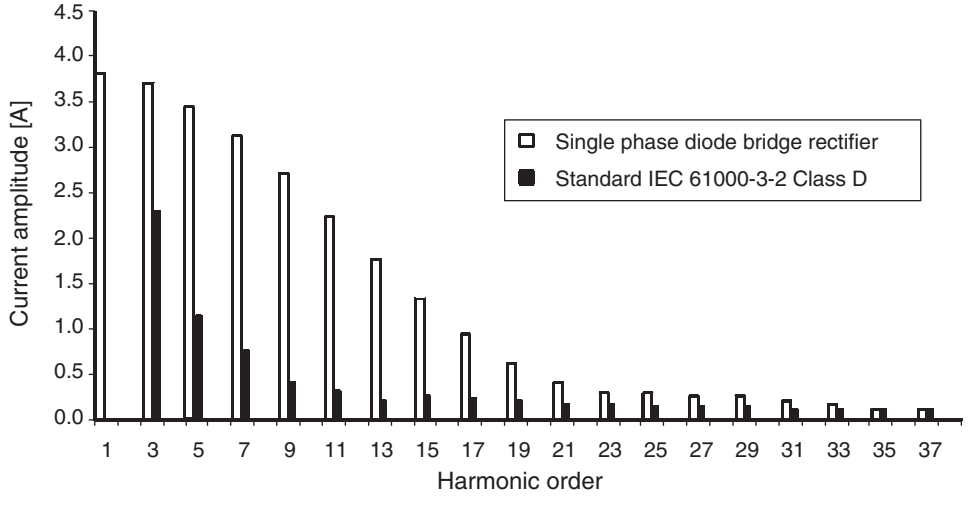

FIGURE 11.16 Input current harmonics produced by a single-phase diode bridge rectifier.

11.3 Unity Power Factor Single-phase Rectifiers

11.3.1 The Problem of Power Factor in Single-phase Line-commutated Rectifiers

The main disadvantages of the classical line-commutated rectifiers are that (i) they produce a lagging displacement factor with respect to the voltage of the utility; (ii) they generate an important amount of input current harmonics.

These aspects have a negative influence on both power factor and power quality. In the last several years, the massive use of single-phase power converters has increased the problems of power quality in electrical systems. In effect, modern commercial buildings have 50% and even up to 90% of the demand, originated by non-linear loads, which are composed mainly by rectifiers [1]. Today it is not unusual to find rectifiers with total harmonic distortion of the current $\text{THD}_i > 40\%$, originating severe overloads in conductors and transformers.

Figure 11.15a shows a single-phase rectifier with a capacitive filter, used in much of today's low-power equipment. The input current produced by this rectifier is illustrated in Fig. 11.15b, it appears highly distorted due to the presence of the filter capacitor. This current has a harmonic content shown in Fig. 11.16 and Table 11.1, with a $\text{THD}_i = 197\%$.

The rectifier in Fig. 11.15 has a very low power factor of $\text{PF} = 0.45$, due mainly to its large harmonic content.

TABLE 11.1 Harmonic content of the current of Fig. 11.15

n	3	5	7	9	11	13	15	17	19	21
I_n/I_1 [%]	96.8	90.5	81.7	71.0	59.3	47.3	35.7	25.4	16.8	10.6

11.3.2 Standards for Harmonics in Single-phase Rectifiers

The relevance of the problems originated by harmonics in single-phase line-commutated rectifiers has motivated some agencies to introduce restrictions to these converters. The IEC 61000-3-2 Class D International Standard establishes limits to all low-power single-phase equipment having an input current with a "special wave shape" and an active input power $P \leq 600\,\text{W}$. Class D equipment has an input current with a special wave shape contained within the envelope given in Fig. 11.15b. This class of equipment must satisfy certain harmonic limits, shown in Fig. 11.16. It is clear that a single-phase line-commutated rectifier with the parameters shown in Fig. 11.15a is not able to comply with the standard IEC 61000-3-2 Class D. The standard can be satisfied only by adding huge passive filters, which increases the size, weight, and cost of the rectifier. This standard has been the motivation for the development of active methods to improve the quality of the input current and, consequently, the power factor.

11.3.3 The Single-phase Boost Rectifier

One of the most important high power factor rectifiers, from a theoretical and conceptual point of view, is the so-called single-phase boost rectifier, shown in Fig. 11.17a, which is obtained from a classical non-controlled bridge rectifier, with the addition of transistor T, diode D, and inductor *L*.

11.3.3.1 Working Principle, Basic Concepts

In boost rectifiers, the input current $i_s(t)$ is controlled by changing the conduction state of transistor T. When transistor T is in the on-state, the single-phase power supply is short-circuited through the inductance *L*, as shown in Fig. 11.17b; the diode D avoids the discharge of the filter capacitor *C* through the transistor. The current of the inductance i_L is given by the following equation

$$\frac{di_L}{dt} = \frac{v_L}{L} = \frac{|v_s|}{L} \tag{11.26}$$

Due to the fact that $|v_s| > 0$, the on-state of transistor T always produces an increase in the inductance current i_L and consequently an increase in the absolute value of the source current i_s.

When transistor T is turned off, the inductor current i_L cannot be interrupted abruptly and flows through diode D, charging capacitor *C*. This is observed in the equivalent circuit of Fig. 11.17c. In this condition, the behavior of the inductor current is described by

$$\frac{di_L}{dt} = \frac{v_L}{L} = \frac{|v_s| - v_o}{L} \tag{11.27}$$

If $v_o > |v_s|$, which is an important condition for the correct behavior of the rectifier, then $|v_s| - v_o < 0$, and this means that in the off-state the inductor current decreases its instantaneous value.

11.3.3.2 Continuous Conduction Mode (CCM)

With an appropriate firing pulse sequence is applied to transistor T, the waveform of the input current i_s can be controlled to follow a sinusoidal reference, as can be observed in the positive half-wave of i_s in Fig. 11.18. This figure shows the reference

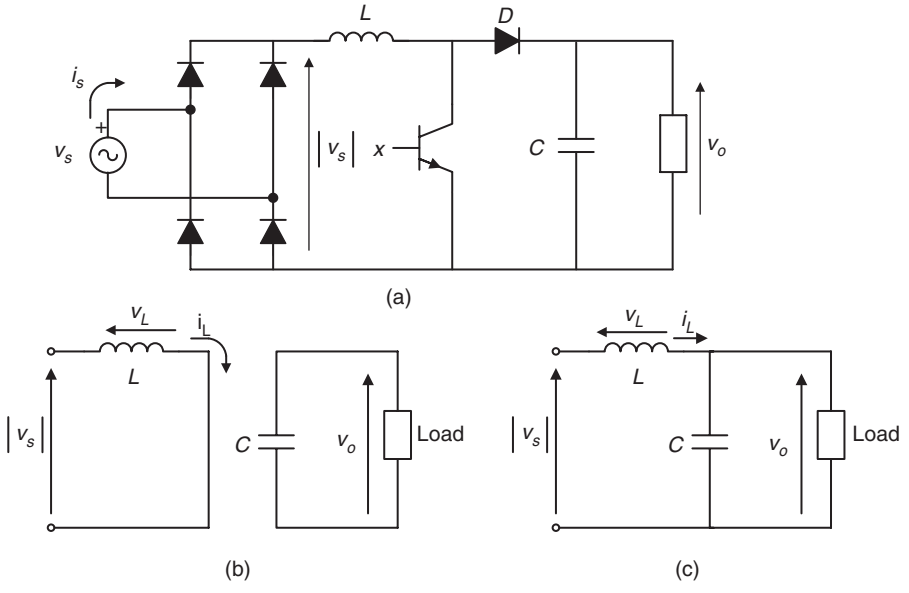

FIGURE 11.17 Single-phase boost rectifier: (a) power circuit and equivalent circuit for transistor T in; (b) on-state; and (c) off-state.

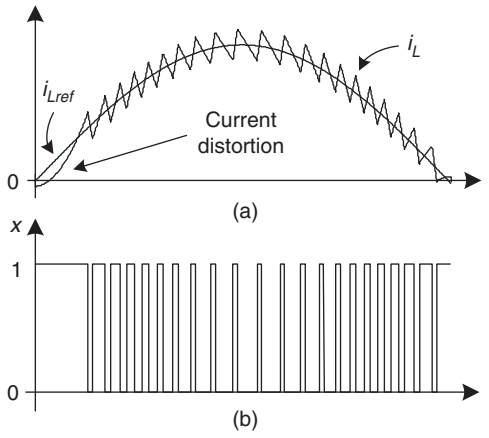

FIGURE 11.18 Behavior of the inductor current i_L: (a) waveforms and (b) transistor T gate drive signal x.

inductor current i_{Lref}, the inductor current i_L and the gate drive signal x for transistor T. Transistor T is on when $x = 1$ and it is off when $x = 0$.

Figure 11.18 clearly shows that the on- (off-) state of transistor T produces an increase (decrease) in the inductor current i_L.

Note that for low values of v_s the inductor does not have enough energy to increase the current value, for this reason it presents a distortion in their current waveform as shown in Fig. 11.18a.

Figure 11.19 presents a block diagram of the control system for the boost rectifier, which includes a proportional-integral (PI) controller, to regulate the output voltage v_o. The reference value i_{Lref} for the inner current control loop is obtained from the multiplication between the output of the voltage controller and the absolute value $|v_s(t)|$. A hysteresis controller provides a fast control for the inductor current i_L, resulting in a practically sinusoidal input current i_s.

Typically, the output voltage v_o should be at least 10% higher than the peak value of the source voltage $v_s(t)$, in order to assure good dynamic control of the current. The control works with the following strategy: a step increase in the reference voltage v_{oref} will produce an increase in the voltage error $v_{oref} - v_o$ and an increase of the output of the PI controller, which originates an increase in the amplitude of the reference current i_{Lref}. The current controller will follow this new reference and will increase the amplitude of the sinusoidal input current i_s, which will increase the active power delivered by the single-phase power supply, producing finally an increase in the output voltage v_o.

Figure 11.20a shows the waveform of the input current i_s and the source voltage v_s. The ripple of the input current can be reduced by shortening the hysteresis width δ. The tradeoff for this improvement is an increase in the switching frequency, which is proportional to the commutation losses of the transistors. For a given hysteresis width δ, a reduction of inductance L also produces an increase in the switching frequency. As can be seen, the input current presents a third-harmonic component. This harmonic is generated by the second-harmonic component present in v_o, which is fed back through the voltage (PI) controller and multiplied by the sinusoidal waveform, generating a third-harmonic component on i_{Lref}. This harmonic contamination can be avoided by filtering the v_o measurement with a lowpass filter or a bandstop filter around $2\omega_s$. The input current obtained using the measurement filter is shown in Fig. 11.20b. Figure 11.20d confirms the reduction of the third-harmonic component.

However, in both cases, a drastic reduction in the harmonic content of the input current i_s can be observed in the frequency spectrum of Figs. 11.20c and 11.20d. This current fulfills the restrictions established by standard IEC 61000-3-2. The total harmonic distortion of the current in Fig. 11.20a is THD = 7.46%, while the THD of the current of Fig. 11.20b is 4.83%, in both cases a very high power factor, over 0.99, is reached.

Figure 11.21 shows the dc voltage control loop dynamic behavior for step changes in the load. An increase in the load, at $t = 0.3$ [s], produces an initial reduction of the output voltage v_o, which is compensated by an increase in the input current i_s. At $t = 0.6$ [s] a step decrease in the load is applied. The dc voltage controller again adjusts the supply current in order to balance the active power.

11.3.3.3 Discontinuous Conduction Mode (DCM)

This PFC method is based on an active current waveform-shaping principle. There are two different approaches considering fixed and variable switching frequency, both operating principles are illustrated in Fig. 11.22.

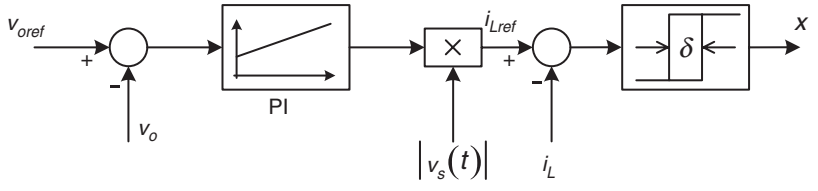

FIGURE 11.19 Control system of the boost rectifier.

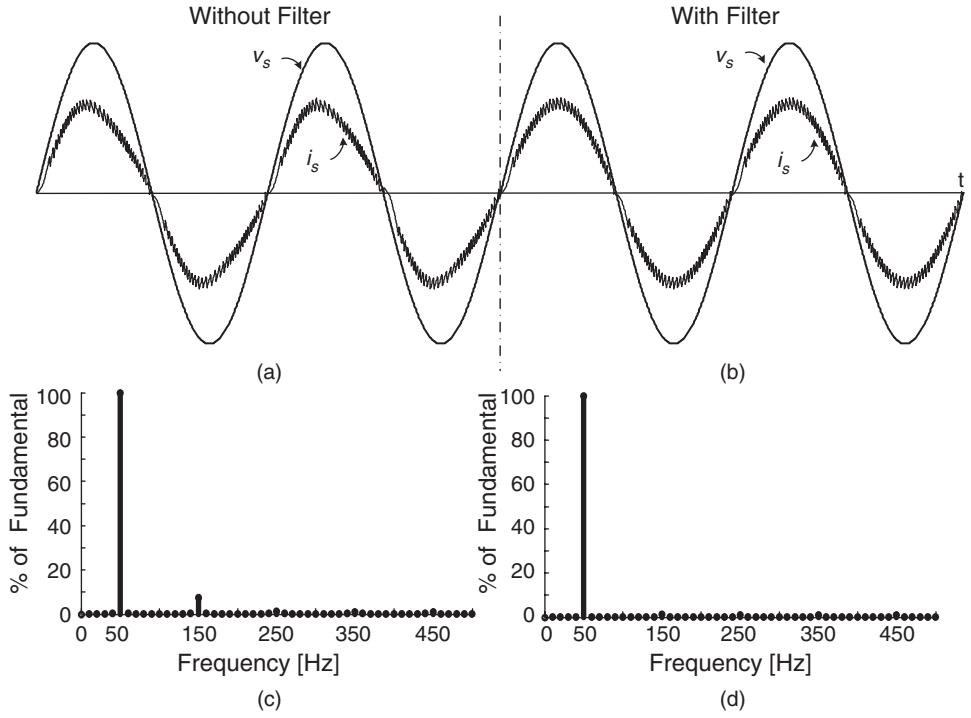

FIGURE 11.20 Input current and voltage of the single-phase boost rectifier: (a) without a filter on v_o measurement; (b) with a filter on v_o measurement; frequency spectrum; (c) without filter; and (d) with filter.

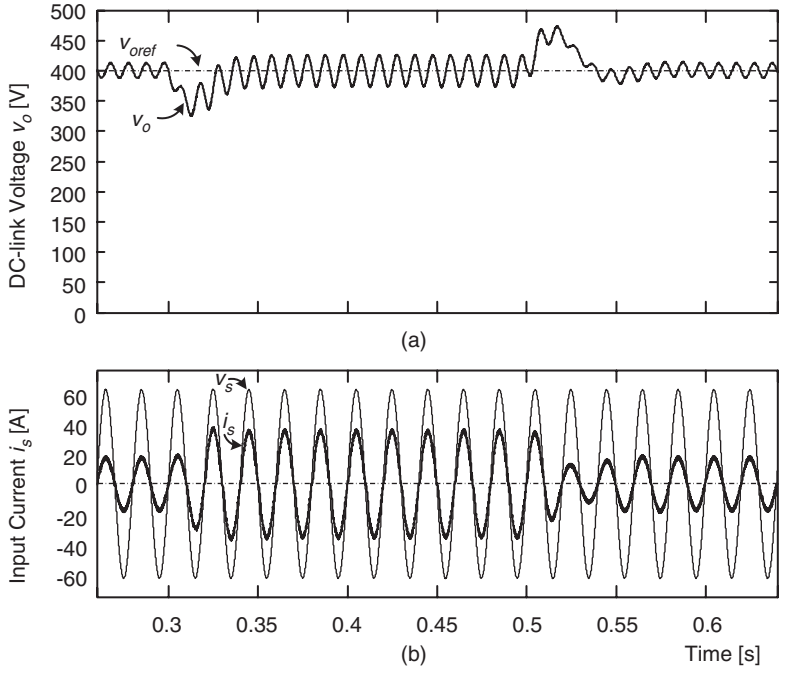

FIGURE 11.21 Response to a change in the load: (a) output-voltage v_o and (b) input current i_s.

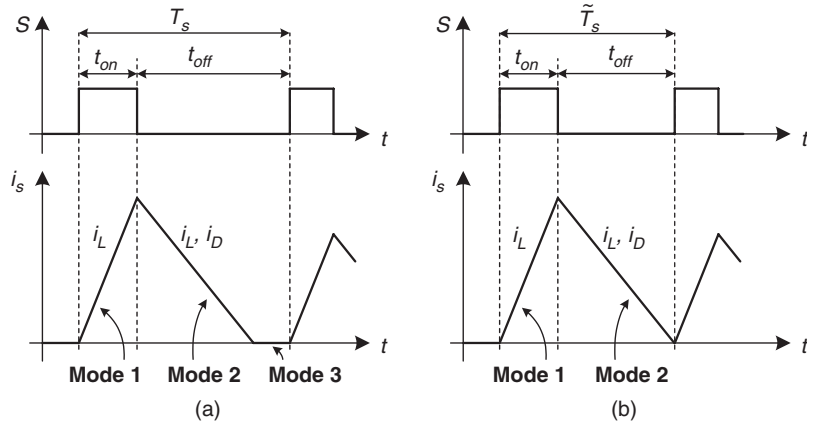

FIGURE 11.22 Boost DCM operating principle: (a) with fixed switching frequency and (b) with variable switching frequency.

a) DCM with Fixed Switching Frequency

The current shaping strategy is achieved by combining three different conduction modes, performed over a fixed switching period T_s. At the beginning of each period the power semiconductor is turned on. During the on-state, shown in Fig. 11.23a, the power supply is short-circuited through the rectifier diodes, the inductor L, and the boost switch T. Hence, the inductor current i_L increases at a rate proportional to the instantaneous value of the supply voltage. As a result, during the on-state, the average supply current i_s is proportional to the supply voltage v_s which yields to power factor correction.

When the switch is turned off, the current flows to the load trough diode D, as shown in Fig. 11.23b. The instantaneous current value decreases (since the load voltage v_o is higher than the supply peak voltage) at a rate proportional to the difference between the supply and load voltage. Finally, the last mode, illustrated in Fig. 11.23c, corresponds to the time in which the current reaches zero value, completing the switching period T_s. Therefore, the supply current is not proportional to the voltage source during the whole control period, introducing distortion and undesirable EMI in comparison to CCM.

The duty cycle $D = t_{on}/T_s$ is determined by the control loop, in order to obtain the desired output power and to ensure operation in DCM, i.e. to reach zero current before the new switching cycle starts. The control strategy can be implemented with analog circuitry as shown in Fig. 11.24, or digitally with modern computing devices. Generally, the duty cycle is controlled with a slow control loop, maintaining the output voltage and duty cycle constant over a half-source cycle.

A qualitative example of the supply voltage and current obtained using DCM is illustrated in Fig. 11.25.

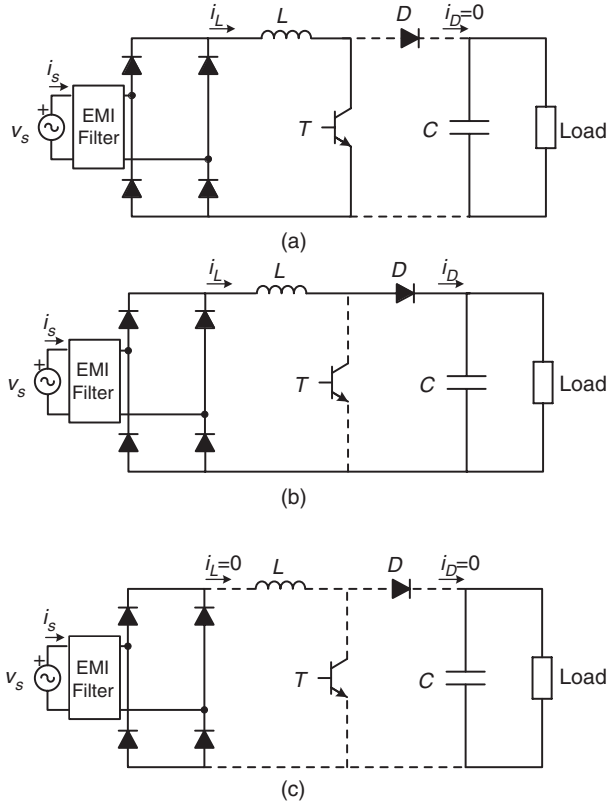

FIGURE 11.23 Boost DCM equivalent circuits: (a) mode 1: transistor on, inductor current increasing; (b) mode 2: transistor off, inductor current decreasing; and (c) mode 3: transistor off, inductor current reaches zero.

b) DCM with Variable Switching Frequency

The operating principle is similar to the one used in the previous case, the main difference is that mode 3 is avoided by switching the transistor again to the on-state, immediately after the inductor current reaches zero value. This reduces the current distortion, with the tradeoff of introducing variable switching frequency (T_s is variable) and consequently lower-order harmonic content.

Both CCM and DCM achieve an improvement in the power factor. The DCM is more efficient since reverse-recovery losses

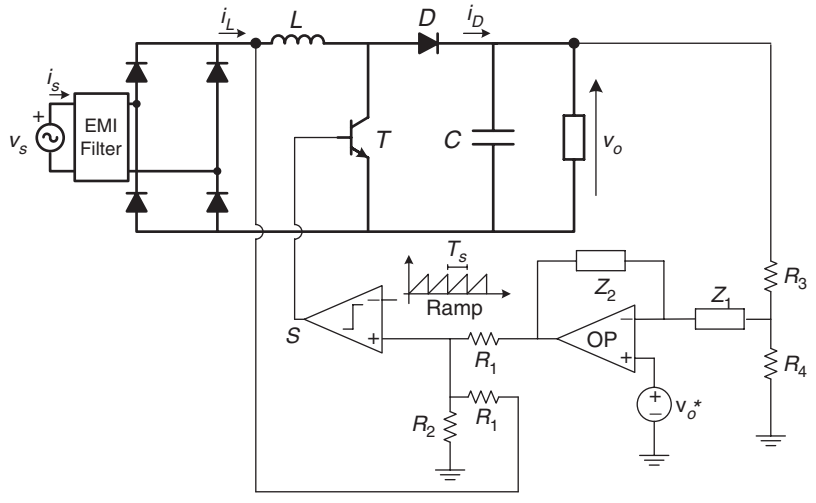

FIGURE 11.24 Boost DCM control circuit with fixed switching frequency.

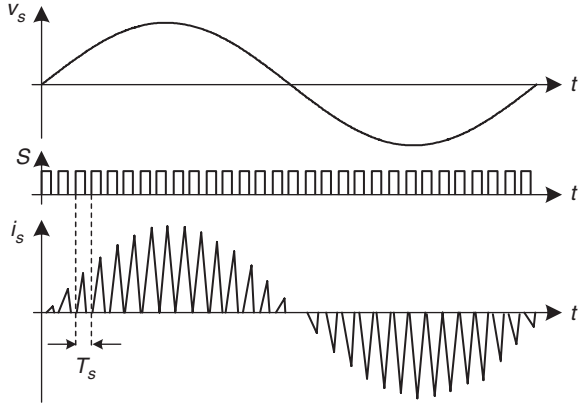

FIGURE 11.25 Boost DCM waveforms: supply voltage, transistor control signal, and supply current.

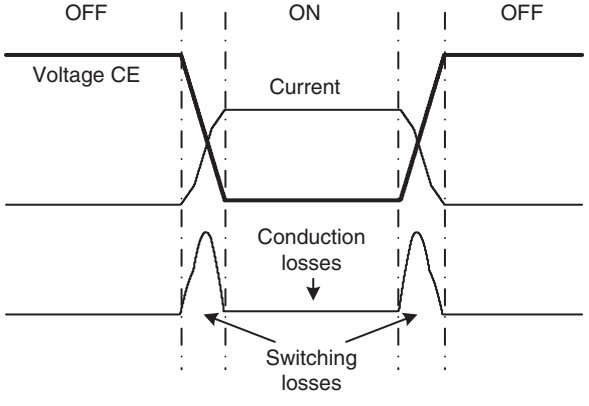

FIGURE 11.26 Conduction and switching losses on a power switch.

of the boost diode are eliminated, however this mode introduces high-current ripple and considerable distortion and usually an important fifth-order harmonic is obtained. Therefore boost-DCM applications are limited to 300 W power levels, to meet standards and regulations. The DCM with variable switching frequency reduces this harmonic content, at expends of a wide distributed current spectrum and all related design problems.

11.3.3.4 Resonant Structures for the Boost Rectifiers

An important issue in power electronics is the power losses in power semiconductors. These losses can be classified in two groups: conduction losses and switching losses, as shown in Fig. 11.26.

The conduction losses are produced by the current through the semiconductor juncture, so these losses are unavoidable. However, the switching losses, which are produced while the power semiconductors work in linear state during the transition from on- to off- state or from off- to on-state, can be reduced or even eliminated, if the switch (transition) occurs when: (a) the current across the power semiconductor is zero; (b) the voltage between the power terminals of the power semiconductor is zero.

This operation mode is used in the so-called *resonant* or *soft-switched* converters, which are discussed in detail in a different chapter of this handbook.

Resonant operation can also be used with the boost converter topology. In order to produce this condition, topology of Fig. 11.17 needs to be modified, by including reactive components and additional semiconductors.

In Fig. 11.27 a resonant structure for zero current switching (ZCS) [2] is shown. As can be seen, additional resonant inductors (L_{r1}, L_{r2}), capacitors (C_r), diodes (D_{r1}, D_{r2}), and power switch (S_r) have been included.

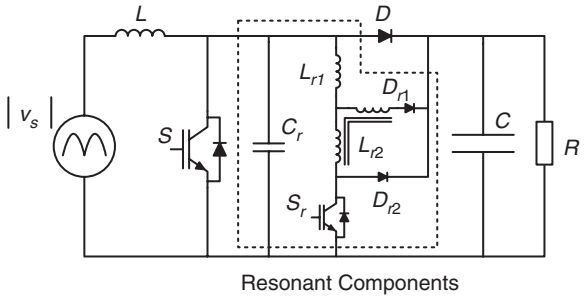

FIGURE 11.27 Boost rectifier with ZCS.

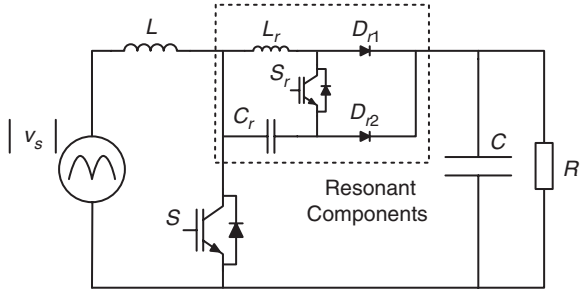

FIGURE 11.28 Boost rectifier with ZVS.

In a similar way, in Fig. 11.28 a resonant structure for zero voltage switching (ZVS) [3] is shown. Once again, additional inductance (L_r), capacitor (C_r), and power switch (S_r) are added, note however, that diode D has been replaced by two "resonant diodes," D_{r1} and D_{r2}.

In both cases, the ZVS or ZCS condition is reached through a proper control of S_r. Other resonant topologies are described in the literature [4–6] with similar behavior.

11.3.3.5 Bridgless Boost Rectifier

The bridgless boost rectifier [7] is shown in Fig. 11.29a. This rectifier replaces the input diode rectifier by a combination of two boost rectifiers which work alternately: (a) when v_s is positive, T_1 and D_1 operate as boost rectifier 1 (Fig. 11.29b); (b) when v_s is negative, T_2 and D_2 operate as boost rectifier 2 (Fig. 11.29c);

This topology reduces the conduction losses of the rectifier [8, 9], but requires a slightly more complex control scheme, also EMI and EMC aspects must be considered.

11.3.4 Voltage Doubler PWM Rectifier

Figure 11.30a shows the power circuit of the voltage doubler pulse width modulated (PWM) rectifier, which uses two transistors T_1 and T_2 and two filter capacitors C_1 and C_2. The transistors are switched complementary to control the waveform of the input current i_s and the output dc voltage v_o. Capacitor voltages V_{C1} and V_{C2} must be higher than the peak value of the input voltage v_s to ensure the control of the input current.

The equivalent circuit of this rectifier with transistor T_1 in the on-state is shown in Fig. 11.30b. For this case, the inductor voltage dynamic equation is

$$v_L = L\frac{di_s}{dt} = v_s(t) - V_{C1} < 0 \qquad (11.28)$$

Equation (11.28) means that under this conduction state, current $i_s(t)$ decreases its value.

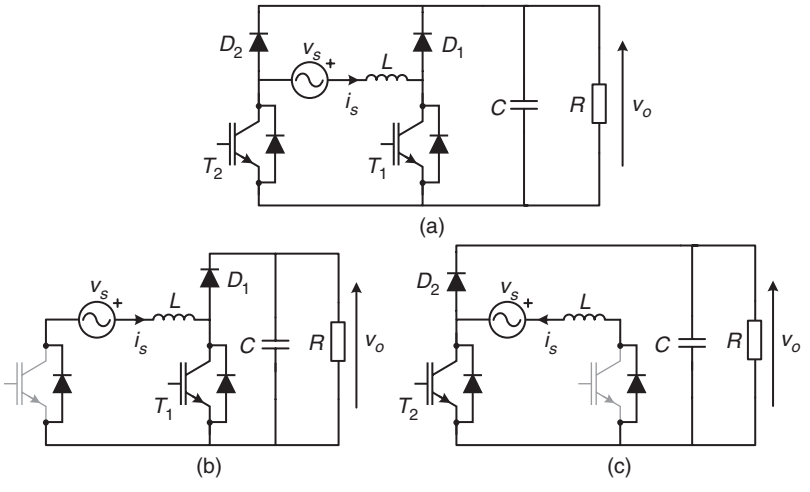

FIGURE 11.29 (a) Power circuit of bridgless boost rectifier; equivalent circuit when; (b) $v_s > 0$; and (c) $v_s < 0$.

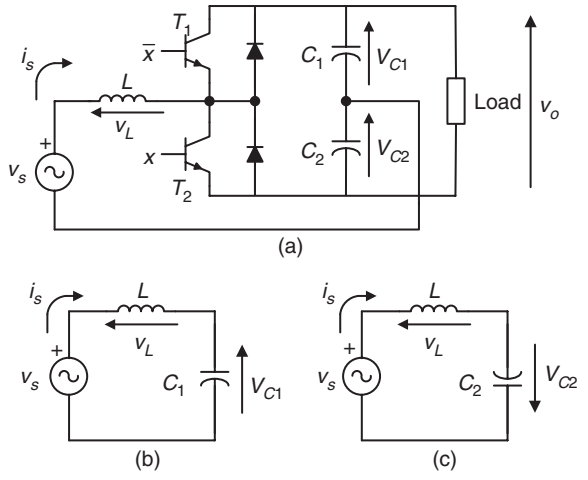

FIGURE 11.30 Voltage doubler rectifier: (a) power circuit; (b) equivalent circuit with T_1 on; and (c) equivalent circuit with T_2 on.

On the other hand, the equivalent circuit of Fig. 11.30c is valid when transistor T_2 is in the conduction state, resulting in the following expression for the inductor voltage

$$v_L = L\frac{di_s}{dt} = v_s(t) + V_{C2} > 0 \qquad (11.29)$$

hence, for this condition, the input current $i_s(t)$ increases.

Therefore the waveform of the input current can be controlled by switching appropriately transistors T_1 and T_2 in a similar way as shown in Fig. 11.18a for the single-phase boost converter. Figure 11.31 shows a block diagram of the control system for the voltage doubler rectifier, which is very similar to the control scheme of the boost rectifier. This topology can present an unbalance in the capacitor voltages V_{C1} and V_{C2}, which will affect the quality of the control. This problem is solved by adding to the actual current value i_s an offset signal proportional to the capacitor's voltage difference.

Figure 11.32 shows the waveform of the input current. The ripple amplitude of this current can be reduced by decreasing the hysteresis width of the controller.

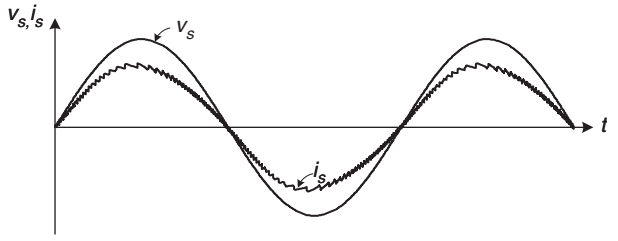

FIGURE 11.32 Waveform of the input current in the voltage doubler rectifier.

11.3.5 The PWM Rectifier in Bridge Connection

Figure 11.33a shows the power circuit of the fully controlled single-phase PWM rectifier in bridge connection, which uses four transistors with antiparallel diodes to produce a controlled dc voltage v_o. Using a bipolar PWM switching strategy, this converter may have two conduction states: (i) Transistors T_1 and T_4 in the on-state and T_2 and T_3 in the off-state; (ii) Transistors T_2 and T_3 in the on-state and T_1 and T_4 in the off-state.

In this topology, the output voltage v_o must be higher than the peak value of the ac source voltage v_s, to ensure a proper control of the input current.

Figure 11.33b shows the equivalent circuit with transistors T_1 and T_4 on. In this case, the inductor voltage is given by

$$v_L = L\frac{di_s}{dt} = v_s(t) - V_0 < 0 \qquad (11.30)$$

Therefore, in this condition a reduction of the inductor current i_s is produced.

Figure 11.33c shows the equivalent circuit with transistors T_2 and T_3 on. Here, the inductor voltage has the following expression

$$v_L = L\frac{di_s}{dt} = v_s(t) + V_0 > 0 \qquad (11.31)$$

which means an increase in the instantaneous value of the input current i_s.

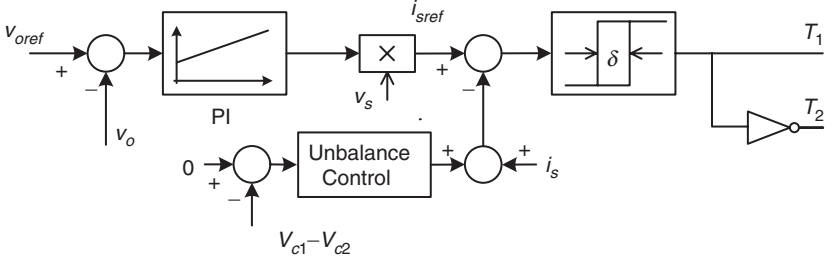

FIGURE 11.31 Control system of the voltage doubler rectifier.

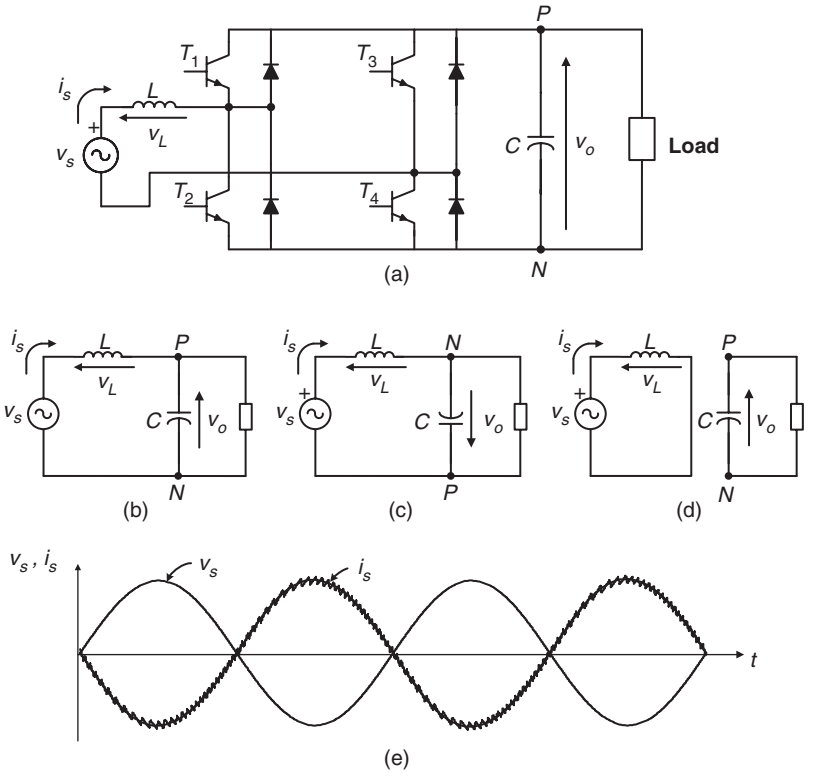

FIGURE 11.33 Single-phase PWM rectifier in bridge connection: (a) power circuit; (b) equivalent circuit with T_1 and T_4 on; (c) equivalent circuit with T_2 and T_3 on; (d) equivalent circuit with T_1 and T_3 or T_2 and T_4 on; and (e) waveform of the input current during regeneration.

Finally, Fig. 11.33d shows the equivalent circuit with transistors T_1 and T_3 or T_2 and T_4 are in the on-state. In this case, the input voltage source is short-circuited through inductor L, which yields

$$v_L = L\frac{di_s}{dt} = v_s(t) + V_0 > 0 \tag{11.32}$$

Equation (11.32) implies that the current value will depend on the sign of v_s.

The waveform of the input current i_s can be controlled by appropriately switching transistors T_1–T_4 or T_2–T_3, originating a similar shape to the one shown in Fig. 11.18a for the single-phase boost rectifier.

The control strategy for the rectifier is similar to the one illustrated in Fig. 11.31, for the voltage doubler topology. The quality of the input current obtained with this rectifier is the same as presented in Fig. 11.32 for the voltage doubler configuration.

The input current waveform can be slightly improved if the state of Fig. 11.33d is used. This can be done by replacing the hysteresis current control with a more complex linear control plus a three-level PWM modulator. This method reduces the semiconductor switching frequency and provides a more defined current spectrum.

Finally, it must be said that one of the most attractive characteristics of the fully controlled PWM converter in bridge connection and the voltage doubler is their regeneration capability. In effect, these rectifiers can deliver power from the load to the single-phase supply, operating with sinusoidal current and a high power factor of PF > 0.99. Figure 11.33e shows that during regeneration, the input current i_s is 180° out of phase with respect to the supply voltage v_s, which means operation with power factor PF ≈ -1 (PF is approximately 1 because of the small harmonic content in the input current).

11.3.6 Applications of Unity Power Factor Rectifiers

11.3.6.1 Boost Rectifier Applications

The single-phase boost rectifier has become the most popular topology for power factor correction (PFC) in general purpose power supplies. To reduce the costs, the complete control system shown in Fig. 11.19 and the gate drive circuit of the power transistor have been included in a single integrated circuit (IC), like the UC3854 [10] or MC33262, shown in Fig. 11.34.

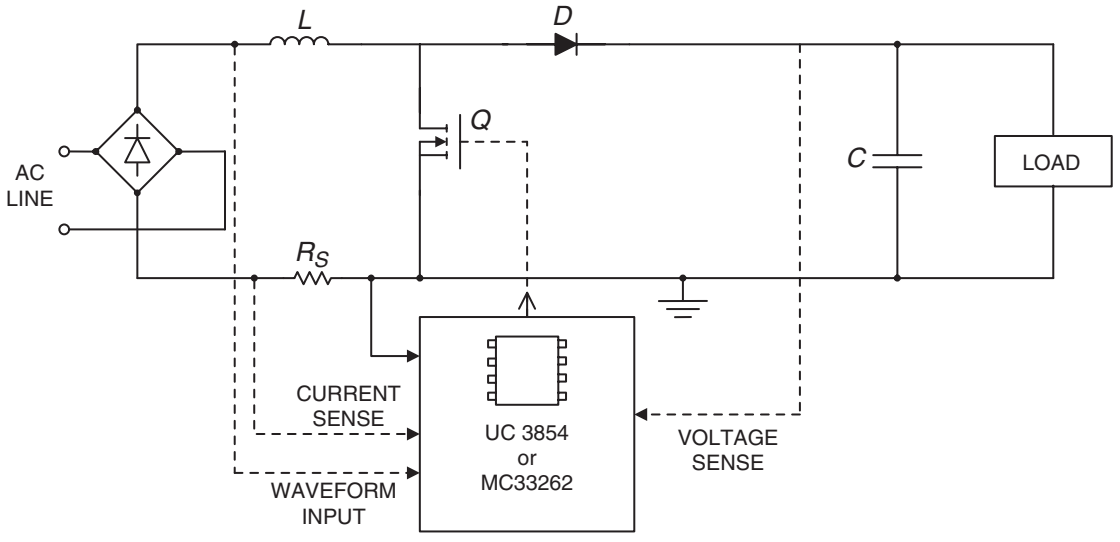

FIGURE 11.34 Simplified circuit of a power factor corrector with control integrated circuit.

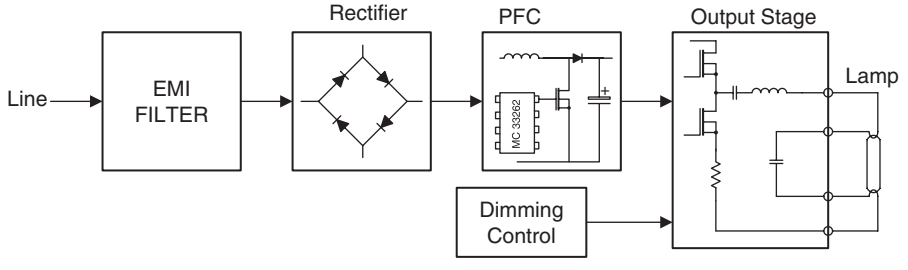

FIGURE 11.35 Functional block diagram of electronic ballast with power factor correction.

Today there is increased interest in developing high-frequency electronic ballasts to replace the classical electromagnetic ballast present in fluorescent lamps. These electronic ballasts require an ac–dc converter. To satisfy the harmonic current injection from electronic equipment and to maintain a high power quality, a high power factor rectifier can be used, as shown in Fig. 11.35 [11].

11.3.6.2 Voltage Doubler PWM Rectifier

The development of low-cost compact motor drive systems is a very relevant topic, particularly in the low-power range. Figure 11.36 shows a low-cost converter for low-power induction motor drives. In this configuration, a three-phase induction motor is fed through the converter from a single-phase power supply. Transistors T_1, T_2 and capacitors C_1, C_2

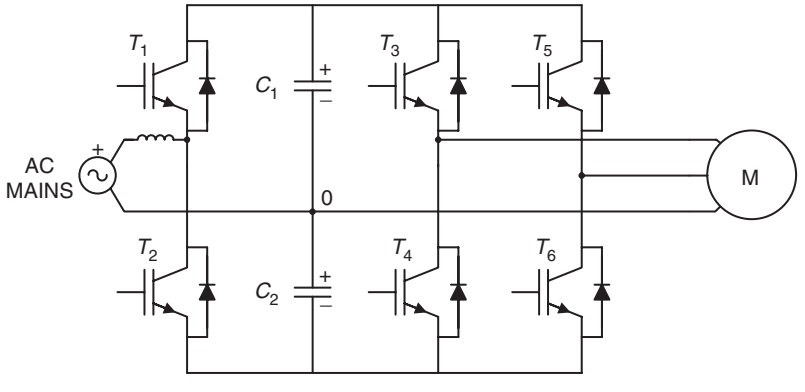

FIGURE 11.36 Low-cost induction motor drive.

constitute the voltage doubler single-phase rectifier, which controls the dc link voltage and generates sinusoidal input current, working with close-to-unity power factor [12]. On the other hand, transistors T_3, T_4, T_5, and T_6 and capacitors C_1 and C_2 constitute the power circuit of an asymmetric inverter that supplies the motor. An important characteristic of the power circuit shown in Fig. 11.36 is the capability of regenerating power to the single-phase mains.

11.3.6.3 PWM Rectifier in Bridge Connection

Distortion of the input current in the line-commutated rectifiers with capacitive filtering is particularly critical in the UPS fed from motor-generator sets. In effect, due to the higher value of the generator impedance, the current distortion can originate an unacceptable distortion on the ac voltage, which affects the behavior of the whole system. For this reason, it is very attractive to use rectifiers with low distortion in the input current.

Figure 11.37 shows the power circuit of a single-phase UPS, which has a PWM rectifier in bridge connection at the input side. This rectifier generates a sinusoidal input current and controls the charge of the battery [13].

Perhaps the most typical and widely accepted area of application of high power factor single-phase rectifiers is in locomotive drives [14]. An essential prerequisite for proper operation of voltage source three-phase inverter drives in modern locomotives is the use of four-quadrant line-side converters, which ensure motoring and braking of the drive, with reduced harmonics in the input current. Figure 11.38 shows a simplified power circuit of a typical drive for a locomotive connected to a single-phase power supply [14], which includes a high power factor rectifier at the input.

Finally, Fig. 11.39 shows the main circuit diagram of the 300 series Shinkansen train [15]. In this application, ac power from the overhead catenary is transmitted through a transformer to single-phase PWM rectifiers, which provide the dc voltage for the inverters. The rectifiers are capable of controlling the input ac current in an approximate sine waveform and in phase with the voltage, achieving power factor close to unity on powering and on regenerative braking. Regenerative braking produces energy savings and an important operational flexibility.

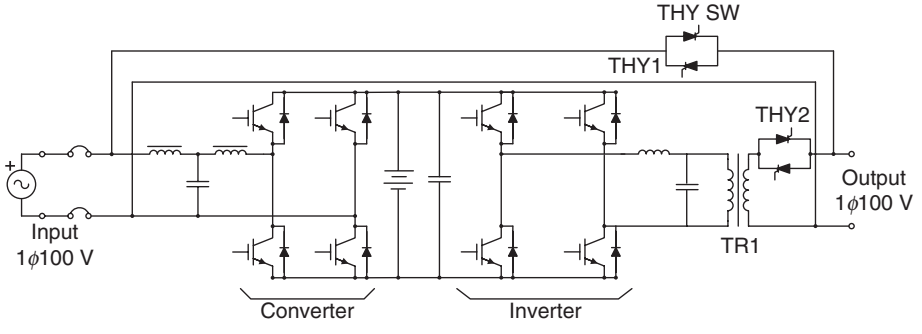

FIGURE 11.37 Single-phase UPS with PWM rectifier.

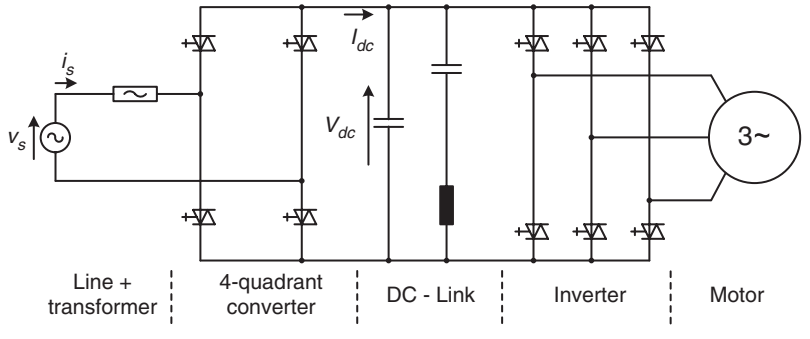

FIGURE 11.38 Typical power circuit of an ac drive for locomotive.

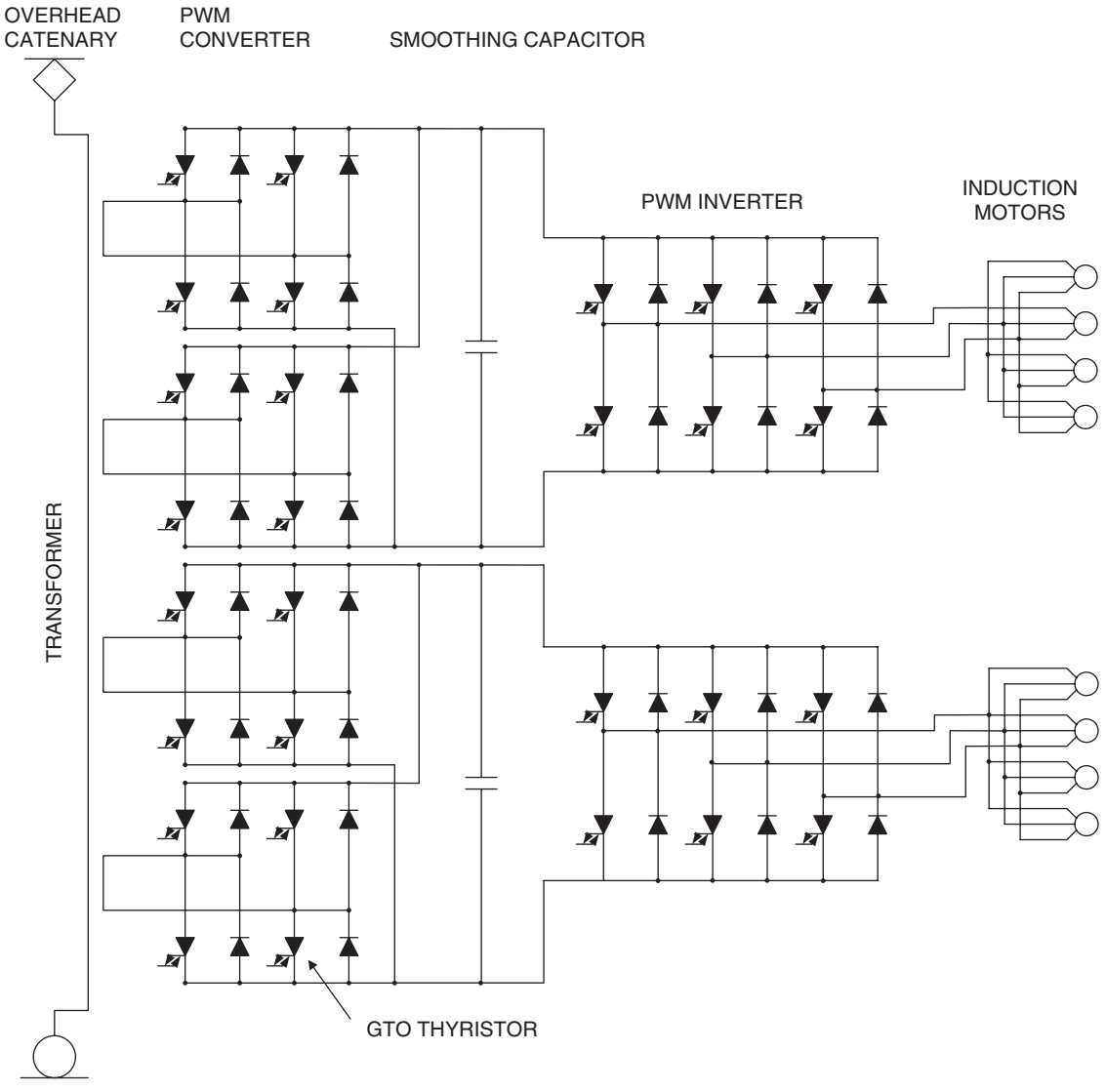

FIGURE 11.39 Main circuit diagram of 300 series Shinkansen locomotives.

Acknowledgment

The authors gratefully acknowledge the valuable contribution of Dr. Rubén Peña, and support provided by the Millennium Science Initiative (ICM) from Mideplan, Chile.

References

1. R. Dwyer and D. Mueller, "Selection of transformers for comercial buildings," in Proc. of IEEE/IAS 1992 Annual Meeting, U.S.A., Oct 1992, pp. 1335–1342.
2. D. C. Martins, F. J. M. de Seixas, J. A. Brilhante, and I. Barbi, "A family of dc-to-dc PWM converters using a new ZVS commutation cell," in Proc. IEEE PESC'93, 1993, pp. 524–530.
3. J. Bassett, "New, zero voltage switching, high frequency boost converter topology for power factor correction," in Proc. INTELEC'95, 1995, pp. 813–820.
4. R. Streit and D. Tollik, "High efficiency telecom rectifier using a novel soft-switched boost-based input current shaper," in Proc. INTELEC'91, 1991, pp. 720–726.
5. Y. Jang and M. M. Jovanovic´, "A new, soft-switched, high-power-factor boost converter with IGBTs," presented at the INTELEC'99, 1999, Paper 8-3.
6. M. M. Jovanovic´, "A technique for reducing rectifier reverse-recovery-related losses in high-voltage, high-power boost converters," in Proc. IEEE APEC'97, 1997, pp. 1000–1007.
7. D. M. Mitchell, "AC-DC converter having an improved power factor," U.S. Patent 4 412 277, Oct 25, 1983.

8. A. F. de Souza and I. Barbi, "A new ZVS-PWM unity power factor rectifier with reduced conduction losses," IEEE Trans. Power Electron, Vol. 10, No. 6, Nov 1995, pp. 746–752.
9. A. F. de Souza and I. Barbi, "A new ZVS semiresonant power factor rectifier with reduced conduction losses," IEEE Trans. Ind. Electron, Vol. 46, No. 1, Feb 1999, pp. 82–90.
10. P. Todd, "UC3854 controlled power factor correction circuit design," Application Note U-134, Unitrode Corp.
11. J. Adams, T. Ribarich, and J. Ribarich, "A new control IC for dimmable high-frequency electronic ballast," IEEE Applied Power Electronics Conference APEC'99, USA,1999, pp. 713–719.
12. C. Jacobina, M. Beltrao, E. Cabral, and A. Nogueira, "Induction motor drive system for low-power applications," IEEE Transactions on Industry Applications, Vol. 35, No. 1. Jan/Feb 1999, pp. 52–60.
13. K. Hirachi, H. Yamamoto, T. Matsui, S. Watanabe, and M. Nakaoka, "Cost-effective practical developments of high-performance 1kVA UPS with new system configurations and their specific control implementations," European Conference on Power Electronics EPE 95, Spain 1995, pp. 2035–2040.
14. K. Hückelheim and Ch. Mangold, "Novel 4-quadrant converter control method," European Conference on Power Electronics EPE 89, Germany 1989, pp. 573–576.
15. T. Ohmae and K. Nakamura, "Hitachi's role in the area of power electronics for transportation," Proc. of the IECON'93. Hawai, Nov 1993, pp. 714–718.